PROCEEDINGS, 45th Workshop on Geothermal Reservoir Engineering
Stanford University, Stanford, California, February 10-12, 2020
SGP-TR-216

Premature Decline of Production Temperature – Can Tracer Test Tell Why?

Horst Behrens, Julia Ghergut, Martin Sauter, Bianca Wagner and Bettina Wiegand

Applied Geoscience Dept., Goldschmidtstr. 3, University of Göttingen, 37077, Germany

iulia.ghergut@geo.uni-goettingen.de

Keywords: thermal breakthrough, permeability window, hydraulic drainage, flow-path shortcut, heat exchange area, effective aperture, tracer test, artificial tracer, residence time, thermal lifetime, piston-flow additive model, advection – dispersion, matrix diffusion

ABSTRACT

For a hydrothermal reservoir operated by means of well-doublet circulation, supposed to deliver at commercial levels for at least four decades and showing, within less than three years since the onset of fluid circulation, a conspicuous decline of production temperature (with no apparent changes in reservoir hydraulics), rapid inter-well drainage or flow-path 'short-circuiting' is being presumed, e. g., by a transmissivity 'window' of either natural origin (falling below detection limits of prior geophysical exploration), or induced by wellbore treatments at very early stages of reservoir development (unintended 'stimulation' resulting in 'misaligned' increase of permeability).

A tracer test was initiated aiming to elucidate the existence and properties of the presumed flow-path shortcut. Interpreting and evaluating the measured tracer signal in terms of solely advective processes (a piston-flow additive model enjoying some popularity) leads to the somewhat paradoxical 'finding' of a (seemingly) unambiguous correlation between the thermal lifetime expectation and the 'measured' fluid residence time, while remaining unable to infer, from the measured tracer signal, the actual size of the presumed transmissivity 'window'. Scoping analytical and numerical simulations of heat and tracer transport by advection-dispersion and matrix diffusion reveal some useful, though limited correlation patterns between temperature decline and tracer breakthrough. Based on such, preliminary findings from the tracer test help constrain the range of plausible properties for the presumed flow-path shortcut.

1. UNEXPECTED TEMPERATURE DROP: PETROTHERMAL, RATHER THAN HYDROTHERMAL?

We deal with a geothermal well doublet in a fractured-porous formation (key data listed in table 1) that had been assessed as 'very promising' and expected to provide for hydrothermal-reservoir operation at commercial levels for at least four decades, but whose rapid decline of production temperature now raises suspicions of a prevailingly petrothermal, rather than hydrothermal behavior. At larger scale, however, evidence to the existence of a hydrothermal resource in this area is beyond doubt – as substantiated by a number of geothermal well doublets and triplets at kilometer scale, operated since years or decades without significant temperature decline, as well as without notable pressure build-up / drawdown at the respective injection / production wells.

Table 1 : Prior, approximate knowledge of hydrothermal reservoir properties

reservoir formation thickness	300 – 400 m
rock matrix porosity	1 – 15 % (ave. transport-effective value: 5 %)
rock matrix permeability	3 – 100 mD (ave. longit. conductivity: 10^{-6} m/s)
rock matrix permeability anisotropy	$K\mathrm{x} \approx 1.5 \times K\mathrm{y} \approx 10 \times K\mathrm{z}$
fractured-porous formation anisotropy	related to major vertical fractures of natural origin (cf. fig. 2 and explanations in section 2)
inter-well distance (n.b.: non-deviated wells)	1 km
length of vertical well-screen intervals	400 m
fluid turnover rate	12,100 m³ / day
initial fluid temperature uphole the production well	~ 150 °C
geo-stratigraphy and geographical location name	cannot be disclosed as yet

Project operators are now presuming some kind of flow-path 'short-circuiting', say, by a transmissivity 'window', of either natural origin (falling short of detection thresholds to prior geophysical exploration), or some other 'connectivity' feature unintendedly induced by wellbore treatments at very early stages of reservoir development (undesirable 'stimulation' resulting in 'misaligned' increase of permeability). A tracer test was initiated aiming to elucidate the existence and characteristics of this putative flow-path shortcut, and tell its effective size. Scoping analytical and numerical simulations of heat and tracer transport by advection – dispersion and matrix diffusion, conducted on a hybrid, fractured-porous reservoir model of simplified geometry and parametrization, are going to reveal some limited, yet useful correlation patterns between temperature decline and tracer breakthrough. Based on such, preliminary findings from the tracer test will help constrain the range of likely properties for the presumed flow-path shortcut.

2. ESTIMATION OF COOLING 'PLUME' SIZE LIMITS, AND MODEL SET-UP FOR FURTHER SIMULATIONS

We first conduct some scoping simulations on heat transport in the *hydrothermal*-reservoir model *without* a shortcut feature. This is supposed to yield an estimation of maximum spatial extent for the cooling 'plume', since any 'short-circuiting' between the wells would lead to a shorter residence time and thus a lower cumulative heat exchange between the rock matrix and the circulating fluid. From this we determine how large a model domain we need to consider in subsequent simulations. Figure 1 samples the simulated cooling 'plume' growth after ten-year operation (under conditions as listed in table 1) in a sequence of reservoir volume slices, with a model domain size that was already reduced accordingly. The location of injection (J) and production (P) screens for the non-deviated (vertical) wells is indicated on the top view of the model domain – which, owing to approximate symmetry (ignoring gravity effects), represents a vertically-halved physical domain, of thickness ½ × 400 m. Slices were cut across and along what were presumed to be some pre-existing major vertical fractures of natural origin (outlined by dashed white lines in fig. 2), striking at 170° counterclockwise from the well doublet 'vector' (J → P). The domain's roughly 3 km² large horizontal section was discretized by 23,000 quadrilateral (mostly non-rectangular) elements, and the flow and transport problem was formulated and solved numerically using finite-element tools provided by FEFLOW5.4 (Diersch, 2014). The latter enables a numerically efficient treatment of major vertical fractures, based on schemes developed by Kolditz (1997) and colleagues.

Inferring the effective aperture of a single, or of distributed fractures (which cannot be told by geophysical exploration methods), from whatever data available, is a non-trivial endeavor. From ancillary simulations, values below 1 mm appear to have negligible effects on reservoir-scale flow and transport. Aperture values exceeding 5 mm, in turn, are geomechanically implausible. For simulations shown here, we assumed a value of 2 mm for the pre-existing (natural-origin) fractures outlined by dashed lines in white, and of 5 mm for the (presumably induced) shortcut feature indicated by solid lines in black in figure 2. One should keep in mind, when interpreting next section's findings, that a certain extent of parameter interplay (fracture aperture versus length, height, position relative to J or P well) persists and cannot be resolved by tracer tests alone.

3. TRACER VERSUS THERMAL BREAKTHROUGH AS A FUNCTION OF SHORTCUT SIZE AND LOCATION

From simulations of temperature decline in the 'short-circuited' reservoir (figures 2 and 3), it turns out that

– the accelerating effect on temperature decline increases monotonously with shortcut length, once its root location determined;

– the presence of a shortcut at the convergent side (P) of the inter-well flow dipole has a stronger accelerating effect on production temperature decline, than a shortcut occurrence of similar size at the divergent (J) side of the dipole;

– jointly, these two monotonicity findings (w. r. to size for fixed root location; w.r. to root location, for fixed size) imply a certain extent of interplay between shortcut size and root location, i. e., neither can be told unambiguously from temperature monitoring alone;

– the shortcut scenario deemed as "i" in fig. 3 (quarter-length shortcut rooted at injection well in fig. 2) is close to what may be regarded as a NOAEL (no-adverse-effect limit level).

The temperature decline actually recorded at the site under investigation, for five years since the start of well-doublet circulation, would plot between the signals labeled "ii" and "p" in figure 3 (solid lines in red and mid-blue), i. e., the shortcut length could range between ¼ and ½ of the inter-well distance, with larger length if rooted at the injection well, and shorter length if rooted at the production well.

Tracer breakthrough simulations (figure 4), on the other hand, show

– the so-called "first arrival" time, i. e., the time at which the tracer signal first exceeds a prescribed detection limit, depends primarily on shortcut length, almost independently of its root location;

– a given-length shortcut produces slightly higher peaks and lower tailings, if rooted at the injection well, than if rooted at the production well;

– for shortcut length values exceeding half of the inter-well distance, the tracer's so-called "first arrival" is seen within less than two weeks, and its signal peak is reached sooner than two months from tracer addition (and, reciprocally, if signal peak occurs before two months, a shortcut extending over more than half the inter-well distance must be assumed – if the aperture (5 mm) and height (400 m) assumptions were valid; mind the parameter interplay!)

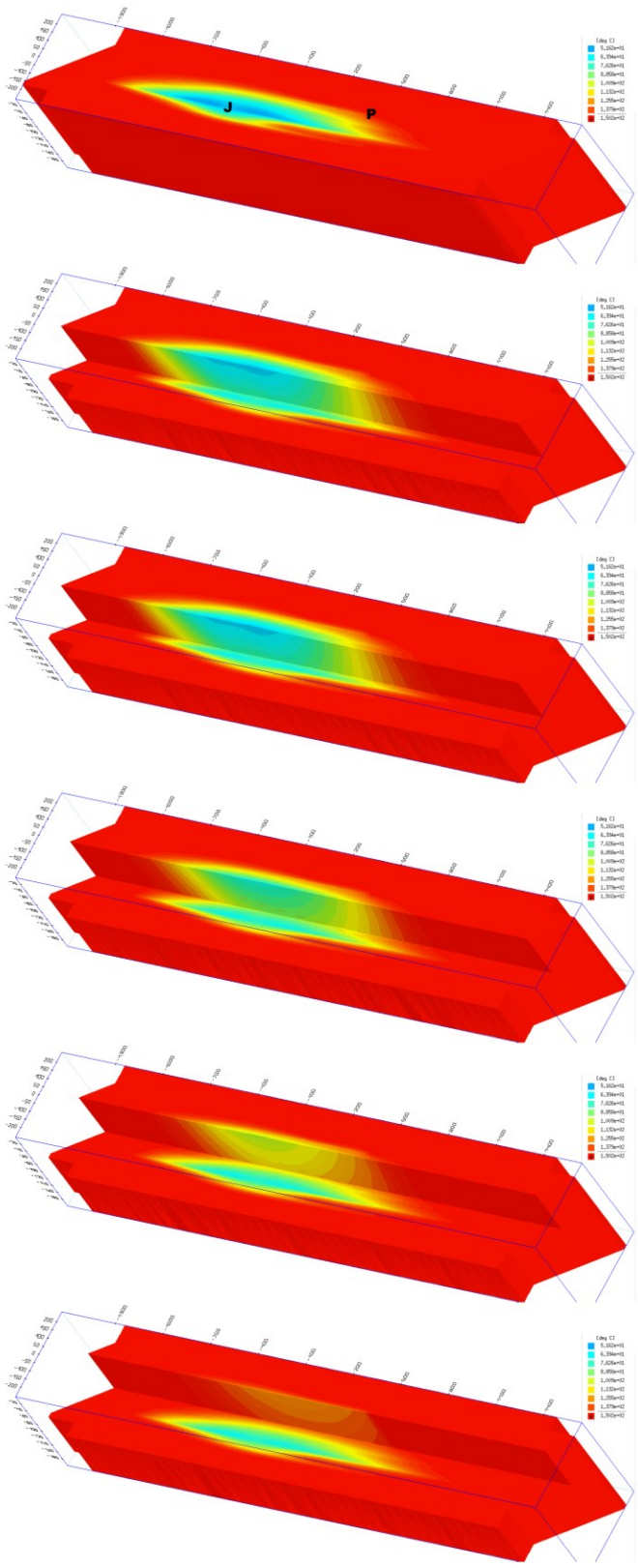

Figure 1: Prior expectations as to ten-year growth of cooling 'plume' within the reservoir. Top view of model (halved physical) domain showing the upper end of injection (J) and production (P) well-screen intervals (in halved formation thickness), followed by 'slice' views with cutting planes across and along what were presumed to be some pre-existing (natural) major vertical fractures (cf. dashed lines in white in fig. 2). Vertical exaggeration factor z:x = z:y = 3

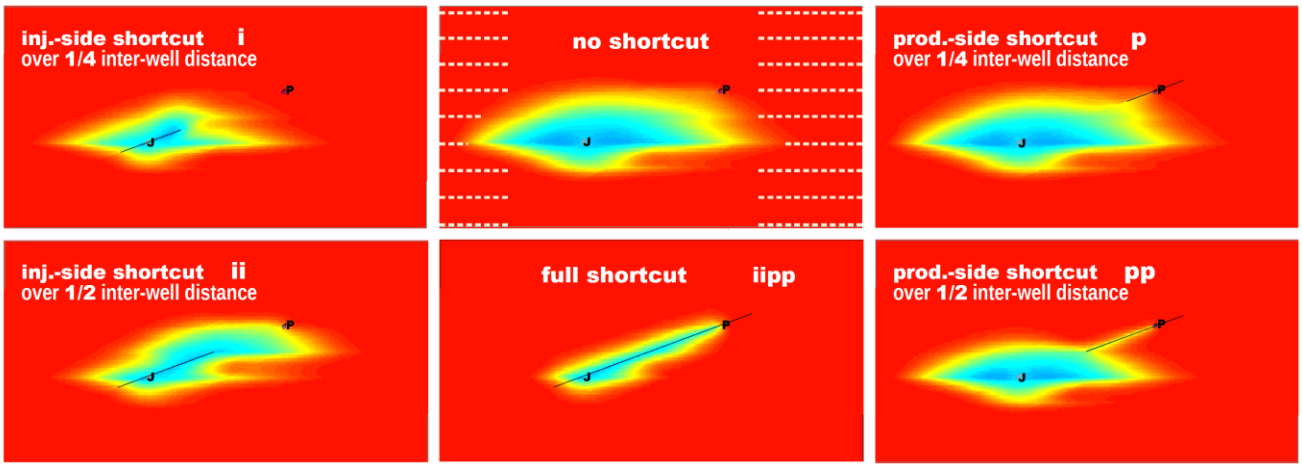

Figure 2: Influence of shortcut length and position (injection- or production-side) on mid-term cooling 'plume' growth. Non-quantitative, intuitive illustration only (reservoir operation stages, i. e. fluid turnover amounts differ between snapshots). Fluid temperature legend like in fig. 1, decreasing from 150 °C (red) to 60 °C (intense blue). Outline of vertical natural fractures (dashed lines in white) shown only for the reference snapshot (of hydrothermal cooling 'plume', without shortcut, after ten years of reservoir operation). Top view with transversal exaggeration factor y:x = 2.5

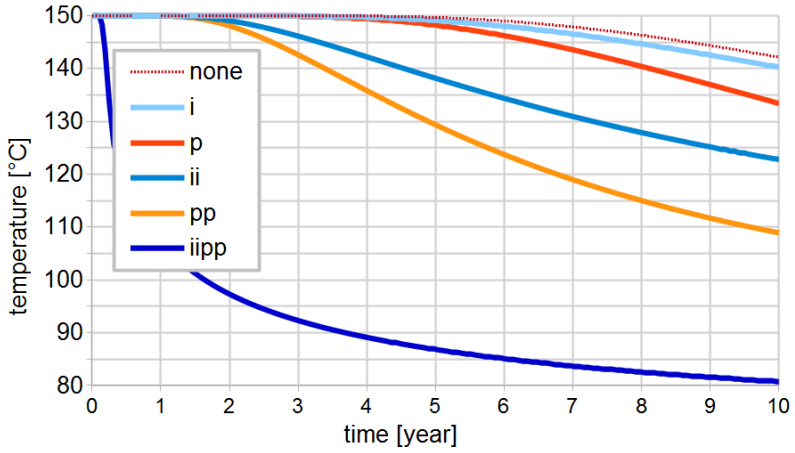

Figure 3: Ten-year temperature decline for the inter-well shortcut scenarios illustrated in fig. 2, assuming a hydraulic and transport-effective aperture of 2 mm for the pre-existing (natural) fractures, and of 5 mm for the shortcut feature.

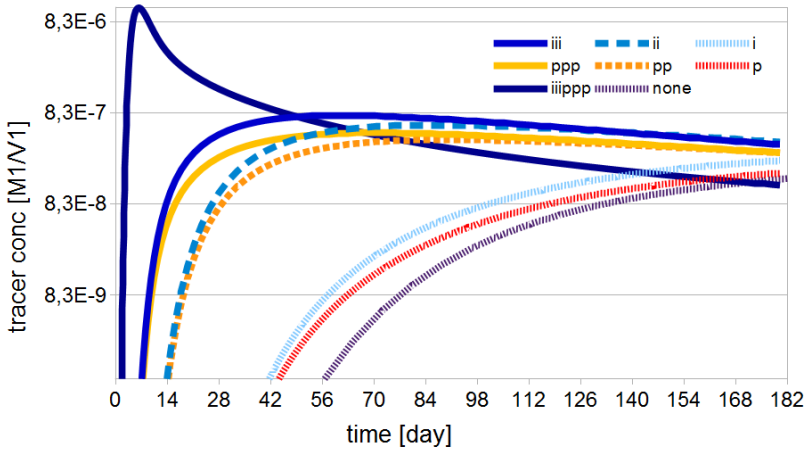

Figure 4: Six-month monitoring of artificial-tracer breakthrough signals for the inter-well shortcut scenarios illustrated in fig. 2, with the same aperture assumptions as in fig. 3.

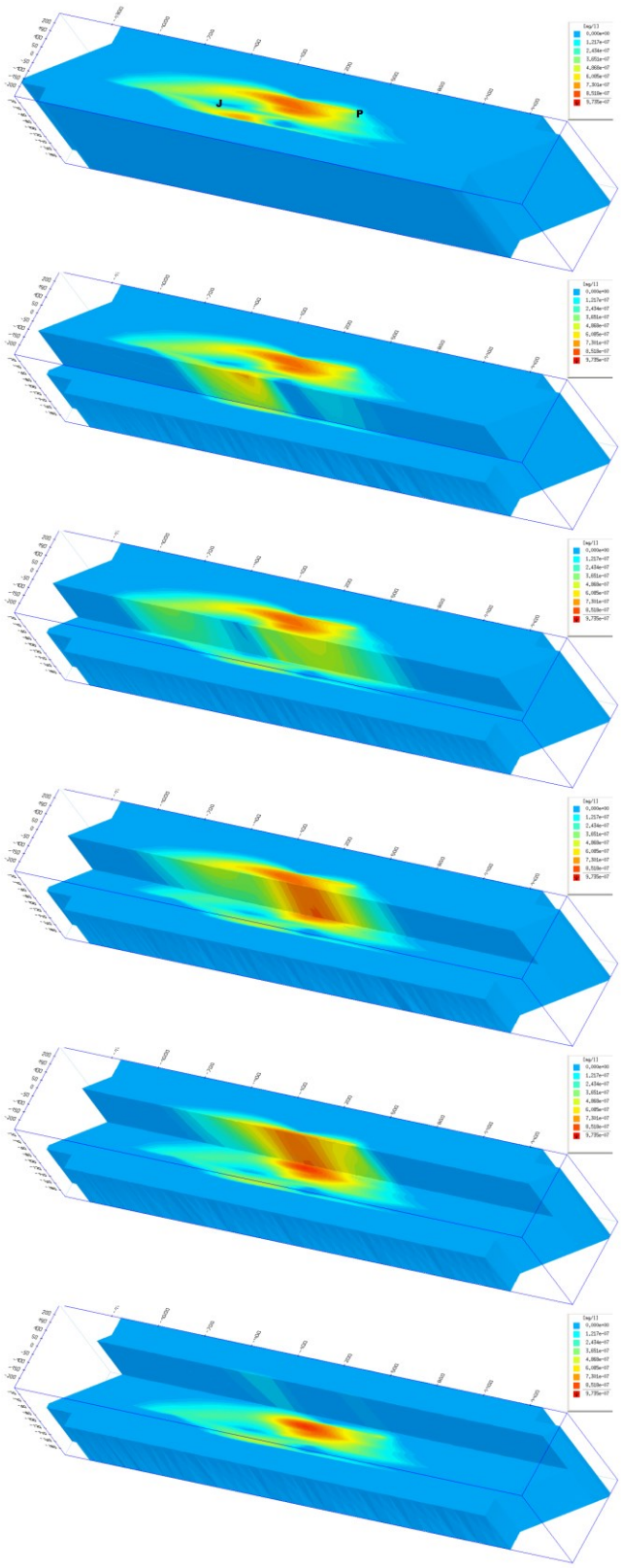

Figure 5: Solute tracer 'plume' persistent within reservoir after six months of continuous fluid turnover (counting since tracer injection). Same top and slice view layout like in fig. 1.

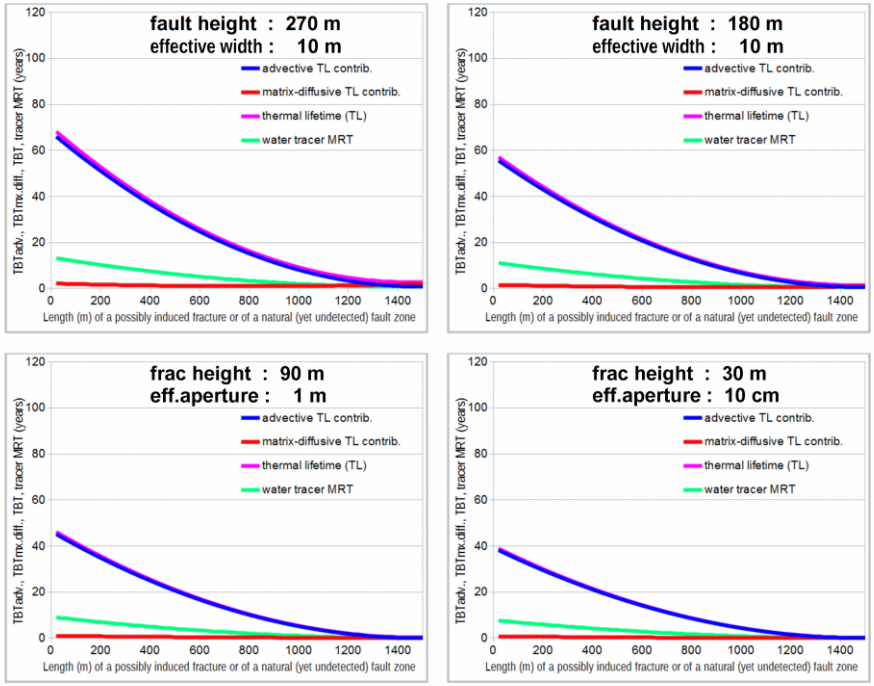

Figure 6: Thermal lifetime (with its advective and matrix-diffusive contributions) and fluid residence time (solely advective 'MRT', according to the piston-flow additive model) as a function of shortcut feature height, length and aperture.

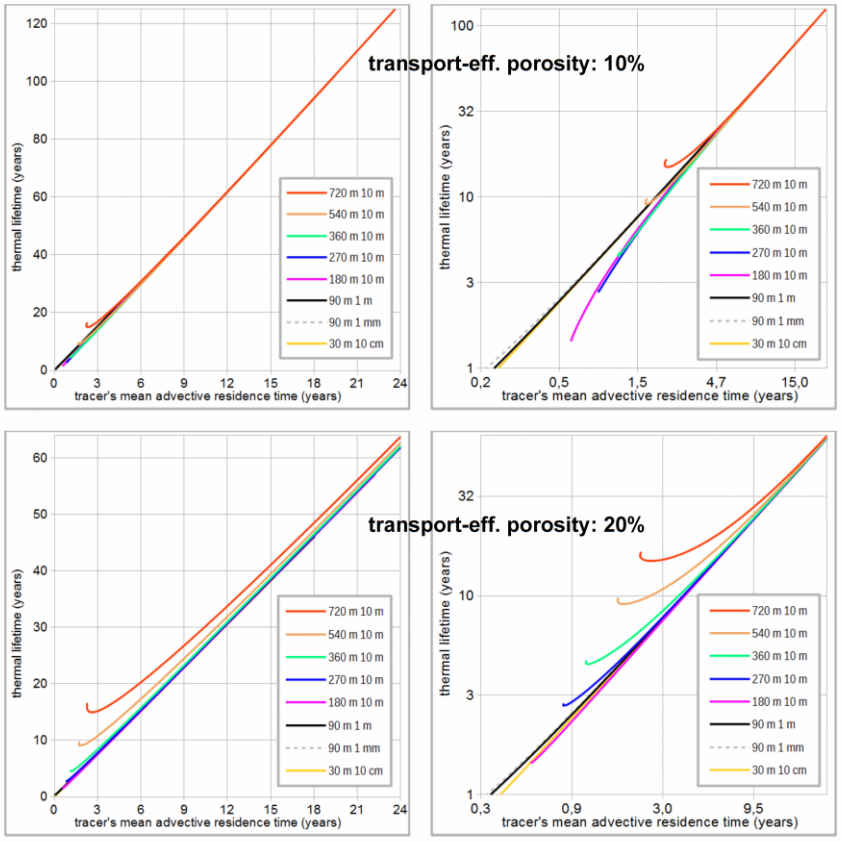

Figure 7: Correlation between fluid advective residence time (according to popular piston-flow additive model) and thermal lifetime expectation (family of parametric plots over shortcut height, length, aperture ranges as sampled in fig. 6).

At the site under investigation, the tracer signal reached a peak value after approx. nine weeks from injection, which would imply a flow-path shortcut of ≤ 500 m length, yet not being able to tell whether it is on the divergent (injection), or the convergent (production) side of the inter-well flow dipole. As a matter of principles, the 'accidentally-stimulated' well (with 'misaligned' transmissivity increase) should become identifiable by hydraulic considerations, but the (somewhat incomplete) pressure data available for this site turn out to be insufficient for elucidation.

4. NON-THERMAL REASONS FOR EARLY THERMAL BREAKTHROUGH – AN ILLUSTRATION

Reasons for misaligned inter-well 'stimulation' may relate to hydrogeomechanical and/or hydrogeochemical processes. The latter may involve a particular textural pattern in the granular structure of the aquifer rock which, when subject to acid treatments, favors channel formation along the inter-well direction (as a preferred direction of channel growth by grain dissolution), thus resulting in faster drainage ('short-cut') between injection and production. As to the former –hydrogeomechanical– processes, let us first recall that with every injection-production well doublet the onset of forced-gradient circulation of fluid will, as illustrated in figures 8 to 12, induce a sequence of coupled hydraulic-geomechanical processes (besides thermal couplings, not addressed here) at different space scales and time stages.

Poroelastic effects will prevail over 'effective stress' changes at early times (immediately following the onset of forced-gradient flow), whereas at later stages the effects of 'effective stress' reduction / augmenting by pore pressure buildup / drawdown around injection / production wells will prevail over poroelastic effects. 'Effective stress' effects look more familiar, including the stabilization tendency around production wells, and the destabilizing (injection-induced seismicity, or stimulation) tendency around injection wells, both propagating away from the wells approximately twice as fast transversally than longitudinally, w. r. to the inter-well axis. This anisotropy is preserved (approximately 2:1) by the δd (MC, MCF) spreading patterns, as easily recognized in the lower part of fig. 8, with d (MC, MCF) denoting Mohr circle's distance from Mohr-Coulomb failure. The poroelastic effects, which prevail at early times, produce a somewhat counter-intuitive picture ('Biot against Terzaghi'), with patterns of longitudinal (i. e., misaligned) 'stimulation' around production wells, and transversal stimulation around injection wells (fig. 8 – upper part, figs. 9 and 10).

Depending on the orientation of pre-existing discontinuities as well as on the values of geomechanical parameters (poroelastic extension of hydraulic diffusivity, friction angle etc.), misaligned 'stimulation' can produce a flow-path short-cut so quickly after the onset of fluid turnover (cf. figs. 9 and 11), that it goes unnoticed from the production well's pressure gauge (if at all available) records. In any case, a significant volume of potential stimulation ($\delta d < 0$, with $|\delta d| \sim$ tens of MPa) connects the injection with the production well *contiguously* at *early* times, comprising a desirable stimulation wing (transversal to the inter-well axis) at the injection well and a misaligned 'stimulation' wing (along the inter-well axis) at the production well. A flow-path short-cut occurring along the latter at early times, and staying open at subsequent times (even when δd becomes >0) by virtue of shear displacement, may be sufficient to explain the premature temperature drop at the production well (cf. scenarios 'p', 'pp' in figs. 2 – 3), but it will not occur automatically for every geothermal-well doublet, since a number of particular circumstances must further be met.

For the particular site under consideration, one may wish to also account for the effects of neighboring wells that are being operated within different geothermal projects, as outlined in figures 9 to 12. 'Our' geothermal doublet is denoted by P and J (production and injection well) and, out of >7 surrounding active wells, the more or less closer neighbors P', J' and J'' can be recognized to have some (non-negligible) effect on δd (MC, MCF) for 'our' doublet (compared to the case of a single, isolated same-size doublet placed in a reservoir of infinite extension, under the same NF regime etc., like in fig. 8), besides the more obvious, hydraulic competition effects: the flow catchment volume of P being reduced by P', the discharge volume of J being reduced by J' and J'', both reasons rendering the J – P dipole more 'focused' i. e., *reducing the effective reservoir size* for J – P, the more so as J' and J'' have been operating since many years longer than J – P, thus having grown a larger 'repellent' ellipsoid of pressure buildup.

How will the forced-gradient circulation of fluid by the well doublet / ensemble alter the value of d (MC, MCF), with increasing amount of fluid turnover? Assuming the inter-well dipole axis is approximately along σ_h in a normal-faulting regime, the reservoir being else homogeneous and unbounded, contours of δd (MC, MCF) are shown in the horizontal plane (more generally, the $\sigma_2\sigma_3$ plane) approximately containing all well screens, contours being shaded in blue tones where $\delta d > 0$ (stabilization tendency), and in yellow-lime where $\delta d < 0$ (potential for 'stimulation' or 'induced seismicity'). Mono-contours of 'no change' to Mohr circle's distance from failure ($\delta d = 0$) are shown accordingly, delineating between bulk regions of potential stimulation (yellow) or of stabilization tendency (blue). Contours and shadings are not meant to provide a strict quantitative account, thus no numbers or legends are shown; this merely illustrative, semi-analytical calculation (cf. Rudnicki 1986, Altmann 2010) with typical values for fluid turnover rates (cf. table 1), hydraulic diffusivity, Lamé coefficients, a Biot's coupling coefficient value ~0.6 and a friction angle value ~30° yields, for the potential 'stimulation' areas, negative $|\delta d|$ amounts exceeding 30 MPa at very early times, few MPa at mid-late and some 10 kPa at late turnover stages, i. e. more than sufficient for misaligned 'stimulation' in relevant inter-well areas, if suitably oriented discontinuities pre-exist. Additionally, non-zero shear stresses are also seen to occur in what was formerly a principal ($\sigma_2\sigma_3$) stress plane, i. e. the forced-gradient turnover of fluid induces a rotation of the stress tensor.

Roughly speaking, mid – late operation stages appear to be 'Terzaghi-governed', whereas early operation stages turn out to be rather 'Biot-dominated' thus bearing a hazard for misaligned 'stimulation' around the production well.

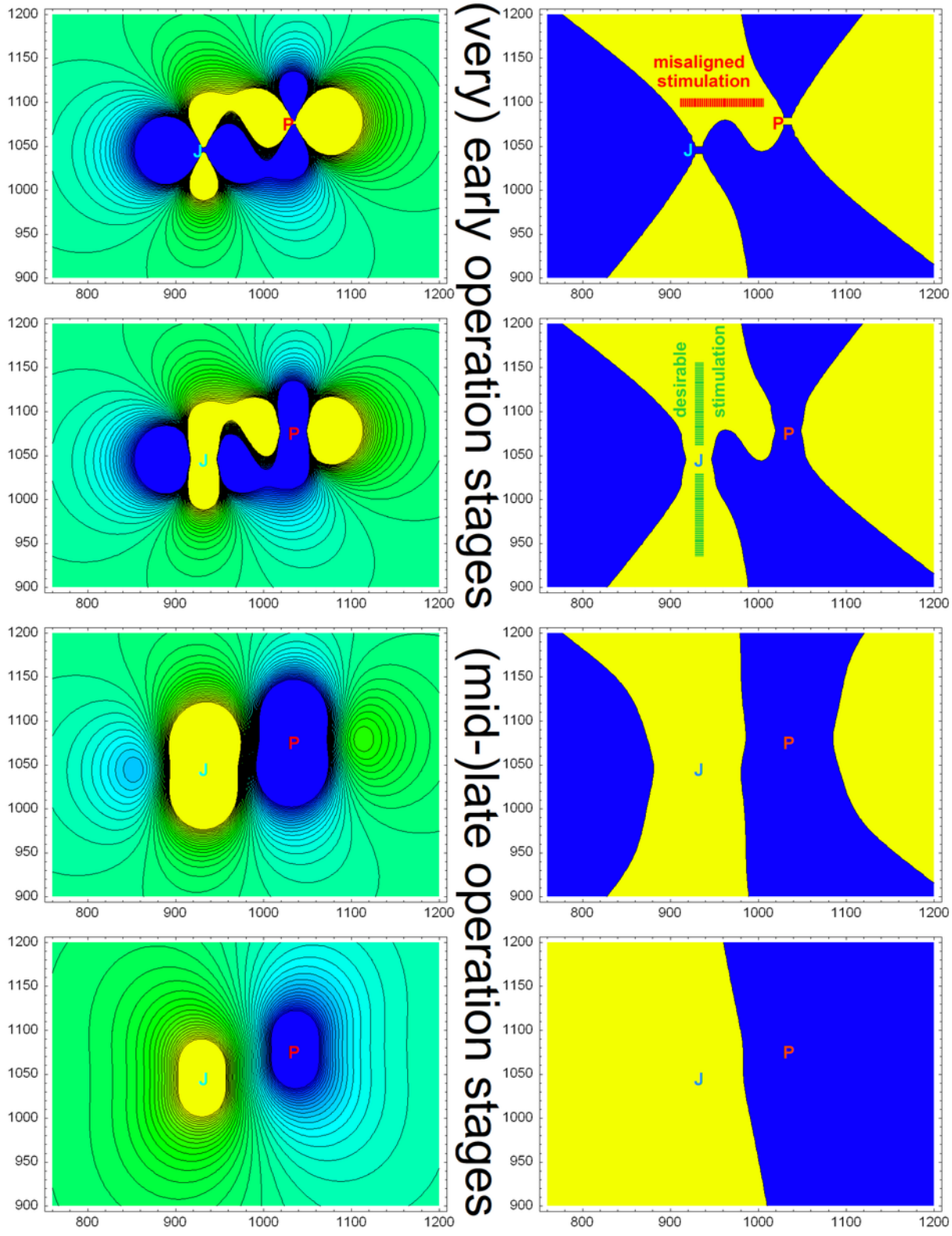

Fig. 8: Fluid-induced changes to Mohr circle's distance from Mohr-Coulomb failure, δd (MC, MCF) for a single geothermal-well doublet in a homogeneous, unbounded reservoir, at four different time stages.

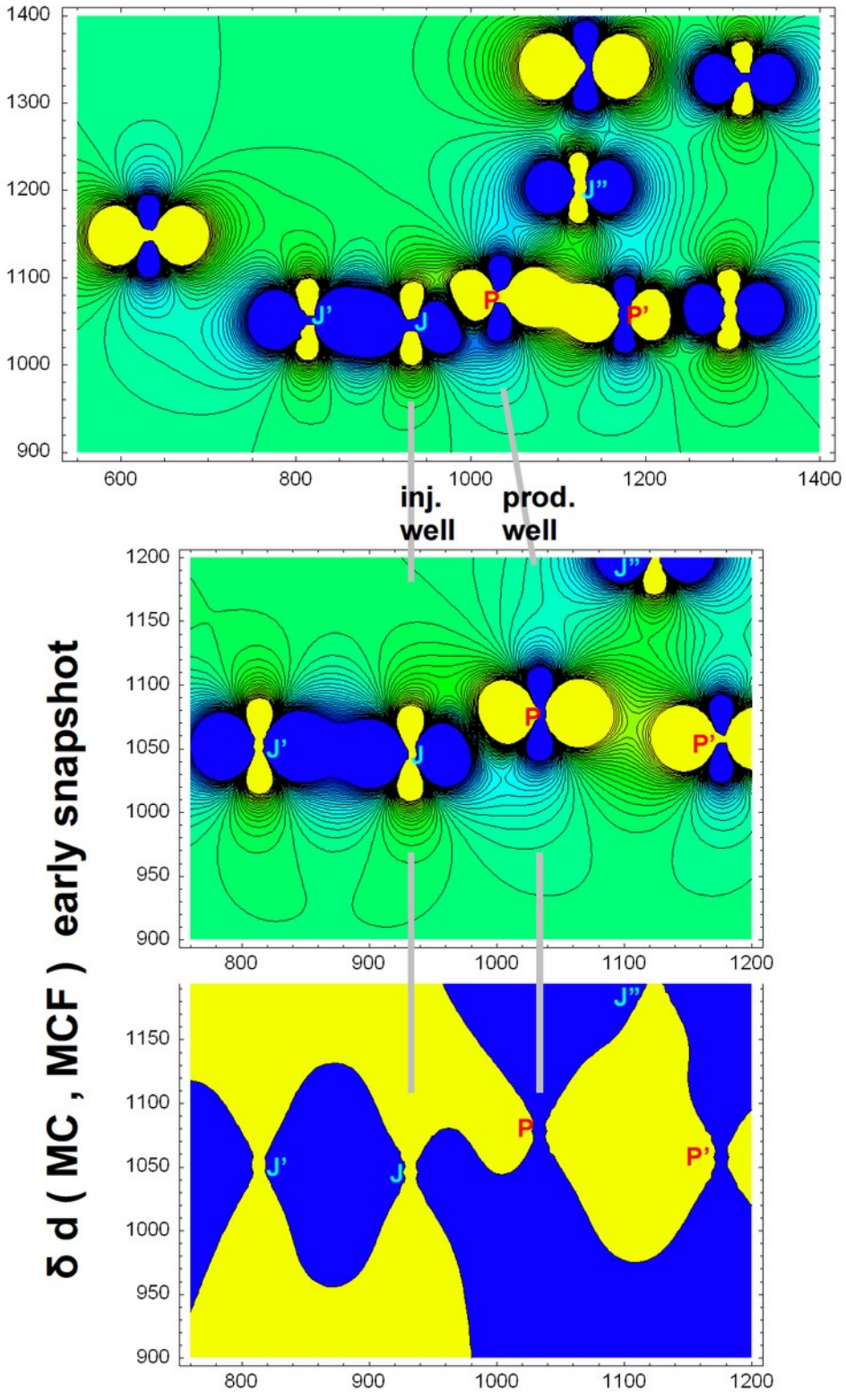

Fig. 9: Fluid-induced changes, δ *d* (MC, MCF) for the same geothermal-well doublet (cf. fig. 8) in a homogeneous, unbounded reservoir, in the presence of 7 further injection and production wells, at a very early stage (immediately following the onset of forced-gradient circulation).

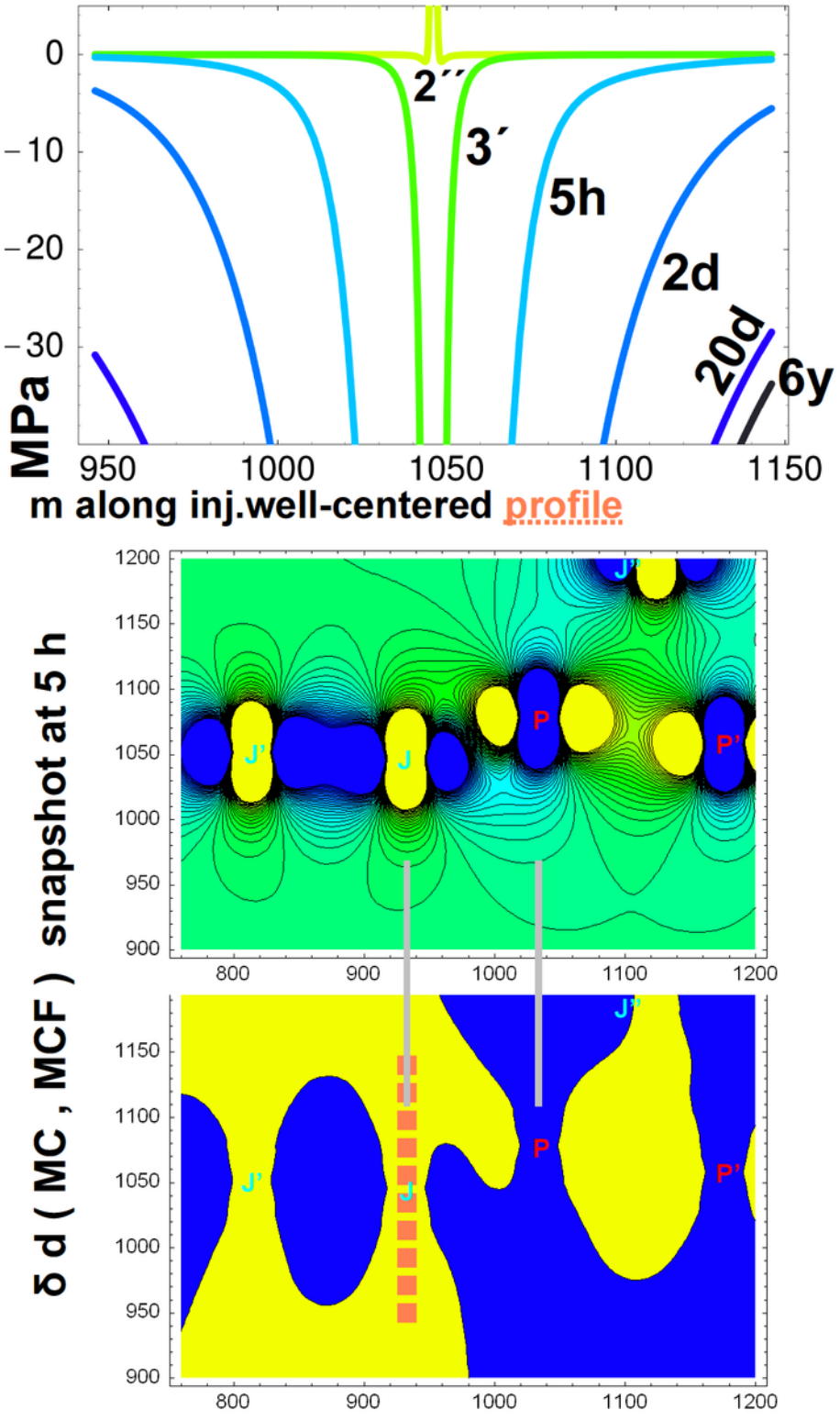

Fig. 10: Fluid-induced changes, δ *d* (MC, MCF) for the same geothermal-well doublet (cf. fig. 8) in a homogeneous, unbounded reservoir, in the presence of 7 further injection and production wells, at early stages, also showing the evolution of δ *d* profiles along a transversal (desirable stimulation) section around the injection well.

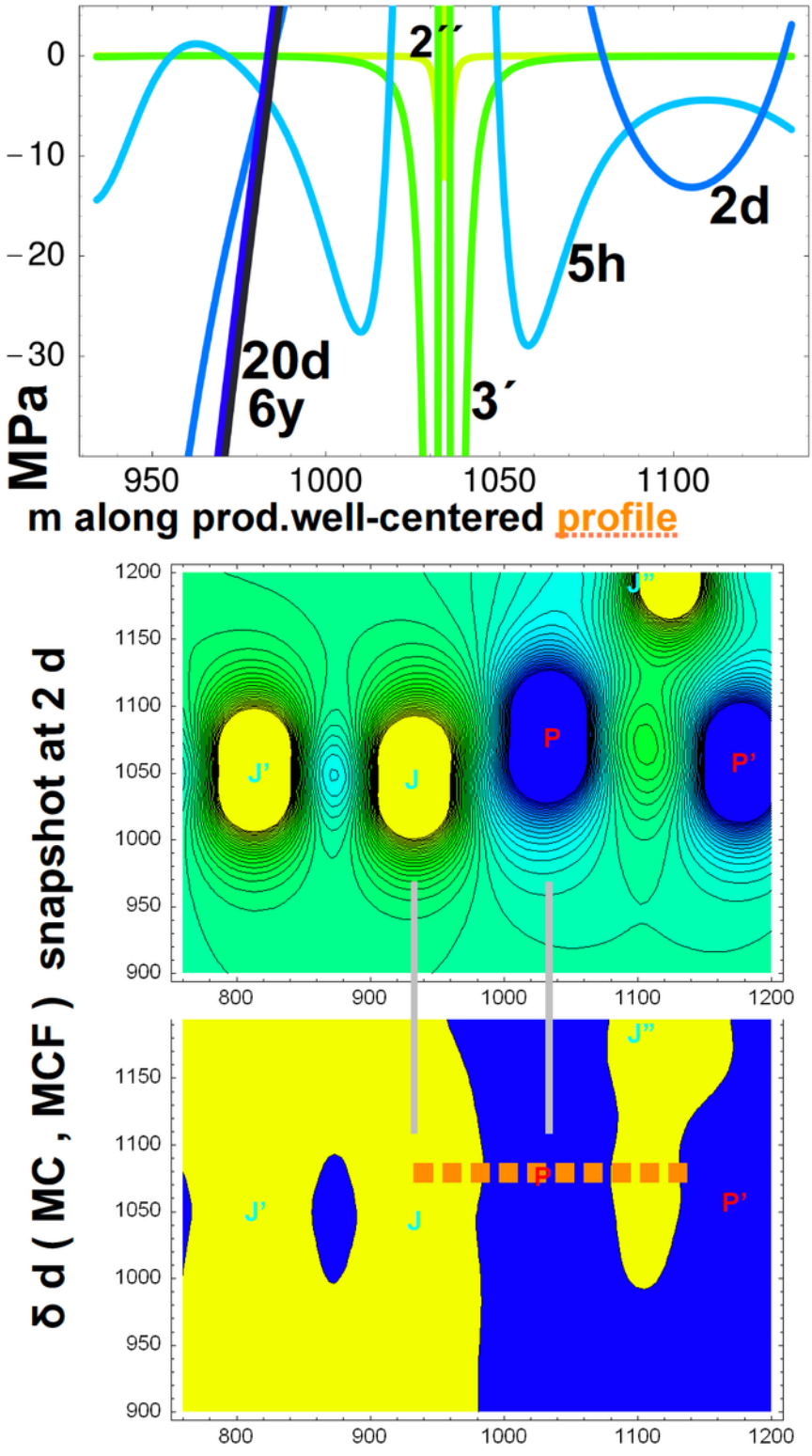

Fig. 11: Fluid-induced changes, δ *d* (MC, MCF) for the same geothermal-well doublet (cf. fig. 8) in a homogeneous, unbounded reservoir, in the presence of 7 further injection and production wells, at mid-late stages, also showing the evolution of δ *d* profiles along a longitudinal (misaligned 'stimulation') section around the production well.

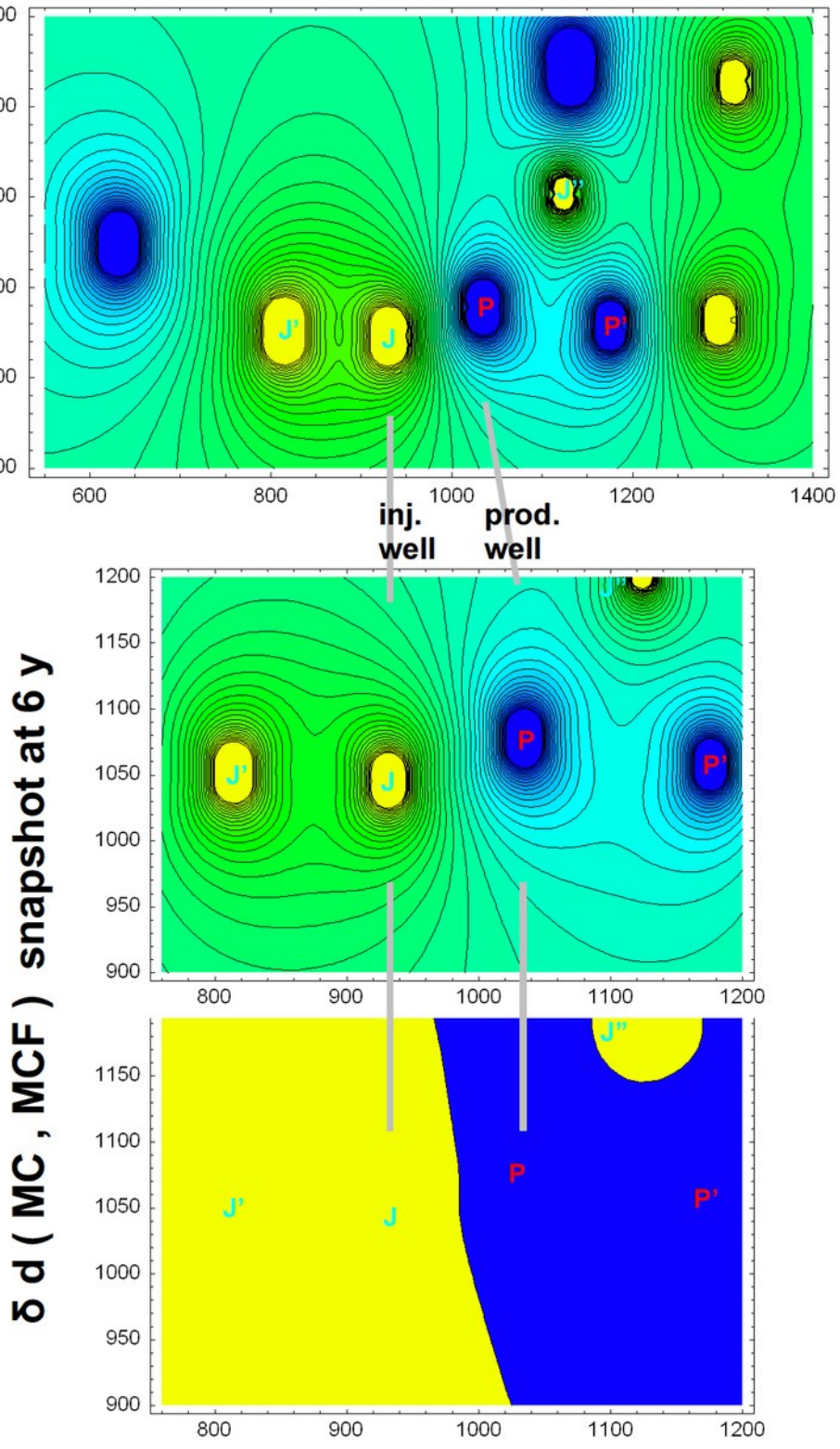

Fig. 12: Fluid-induced changes, δ *d* (MC, MCF) for the same geothermal-well doublet (cf. fig. 8) in a homogeneous, unbounded reservoir, in the presence of 7 further injection and production wells, at late stages of reservoir operation.

5. TWO CAVEATS

In spite of rapid drainage, considerable amounts of tracer remain within the reservoir as a widely-dispersed ‘plume’ (cf. figure 5 for shortcut scenario “ii”, even without considering solute re-circulation by virtue of re-injection, i. e. signal self-convolution). Thus, re-use of the same tracer species for the purpose of further investigations (e. g., after drilling additional wells) within the same or adjacent reservoir volumes is not recommendable.

Interpreting and evaluating the measured tracer signal in terms of solely advective processes (according to a popular piston-flow additive model), as illustrated by figure 6 for parameter ranges significantly wider than considered in figures 1 – 5, leads to the somewhat paradoxical ‘finding’ of a (seemingly) unambiguous correlation (figure 7) between the thermal lifetime expectation and the ‘measured’ fluid residence time, while remaining unable to infer, from the measured tracer signal, the actual size of the presumed transmissivity window or flow-path shortcut. Moreover, solely-advective models do not even assess advection adequately, but tend to strongly over-estimate its velocity. For the short-term transport of a solute tracer, neglecting the effects of matrix diffusion may often be acceptable, but reducing heterogeneous advection in the fractured-porous reservoir to a piston-flow additive process is rarely a suitable approximation. elucidation.

The somewhat counter-intuitive findings illustrated in figures 8 to 10 – e. g., that misaligned ‘stimulation’ is more likely to occur at the production, than at the injection well, by virtue of poroelastic effects at (very) early operation stages – may aid in constraining the range of ambiguity (between ‘i...’ and ‘p...’ scenarios, cf. figures 3 and 4) in temperature and tracer signal interpretation.

Long-term financial support (2014 – 2020) from the German Federal Ministry for Economic Affairs and Energy (BMWi), under grant no. (FKZ) 0325515 is gratefully acknowledged.

REFERENCES

Altmann, J. B.: Poroelastic effects in reservoir modelling. Ph. D. Thesis, Karlsruhe (2010)

Diersch, H.-J. G.: *FEFLOW – Finite-element modeling of flow, mass and heat transport in fractured and porous media*, Springer, Berlin Heidelberg (2014)

Kolditz, O.: *Strömung, Stoff- und Wärmetransport im Kluftgestein*, Gebr. Borntraeger, Berlin Stuttgart (1997)

Rudnicki, J. W.: Fluid mass sources and point forces in linear elastic diffusive solids. *Mechanics of Materials*, **5** (1986), 383-393